Photophysical Processes and Sensor Properties of Multi-colour Fluorescent Polyimides Based on ESIPT and FRET

Atsuko TABUCHI, Teruaki HAYAKAWA, Shigeki KUWATA, Ryohei ISHIGE, and Shinji ANDO*

Dept. Chemistry and Materials Science, Tokyo Institute of Technology,
Ookayama2-12-1-E4-5, Meguro-ku, Tokyo 152-8552, Japan
E-mail: ando.s.aa@m.titech.ac.jp

A semi-aromatic Imide compound (**3TsAPI**) exhibiting multi-colour fluorescent emission via excited-state intramolecular proton transfer (**ESIPT**) and its corresponding acid anhydride (**3TsAPA**) were newly designed and synthesised. 3TsAPA was introduced into the ends of a colourless blue-fluorescent polyimide (PI) and showed bright orange fluorescence at 585 nm with a very large Stokes shift (*SS* = 13,000 $\mathrm{cm^{-1}}$). This emission was achieved via a highly efficient Förster-type resonance energy transfer (**FRET**) from the main chain to the termini This study provides a useful design guideline for imparting multi-colour fluorescence to PIs, which depends on the excitation wavelength derived from the terminal group and the atmosphere while maintaining high thermostability of PIs.

1. Introduction

Fluorescent polyimides (PIs)[1–15] are expected to be applied to solar wavelength conversion films due to their excellent resistance to heat and light and mechanical toughness, and further expansion of the Stokes shift (SS), the difference between absorption and fluorescence wavelengths, and improvement of quantum yield are desired for its practical application. We have therefore designed and synthesised a new excited-state intramolecular hydrogen transfer (**ESIPT**) imide compound with bulky substituents, 3TsAPI (**Figure 1a**).[4] ESIPT is a phenomenon in which the excited state after photo excitation shows long-wavelength fluorescence due to structural stabilisation by intramolecular hydrogen transfer from the *enamine* (**N***) to the *imine* (**T***) form in the excited state. The crystallite of 3TsAPI is white powder under white light, but it exhibits bright orange fluorescence (*SS* = 9,786 $\mathrm{cm^{-1}}$, λ_{em} = 580 nm) in the solid state upon UV irradiation (λ_{ex} = 360 nm) in the solid state with a high fluorescence quantum yield (Φ = 0.22).[4] Depending on the solvent polarity, it also exhibited full-coloured fluorescence from purple to red in organic solutions. Based on quantum chemical TD-DFT calculations, it was elucidated that these phenomena are caused by the competition between the fluorescence emitted from the anionic (**A***) form, in which the hydrogen of the amino group dissociates, in addition to the **N***and **T*** forms (**Figure 2**).

In the present study, a series of end-capped PIs (**ODDC-3TsAPA**, **Figure 1c**) were newly designed and synthesised by introducing a reactive anhydride **3TsAPA** (**Figure 1b**), which has the same core structure as 3TsAPI, at the end of blue-fluorescent PI (**ODDC**) (Fig. 1a), which are colourless under white light, to develop PI films showing red fluorescence, the longest wavelength in the visible region, and their luminescence properties and photophysical processes were investigated.

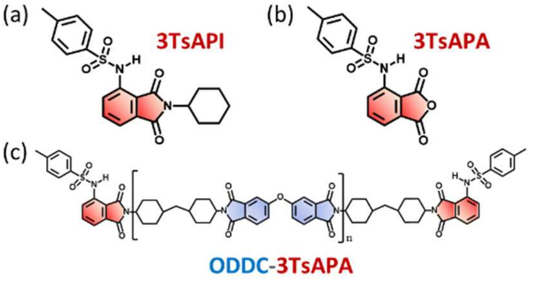

Figure 1 Chemical structures of (a) imide compound (**3TsAPI**), (b) anhydride (**3TsAPA**), and (c) end-capped PI (**ODDC-TsAPA**).

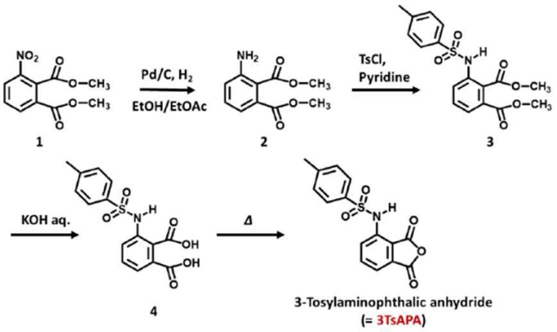

Scheme 1 Synthetic scheme of 3-tosylamino-phthalic anhydride, 3TsAPA (total yield: 18%).

Figure 2 Full-colour fluorescent solvato-chromism of 3TsAPI in various organic solvents (left) and three different states (**N**, **T**, and **A**) generated by solvation and photo-excitation.

2. Experimental

The synthetic route of 3TsAPA is shown in **Scheme 1**. After stirring ODPA and DCHM in DMAc solution under nitrogen atmosphere for 24 h, 3TsAPA was added to ODPA at different end group fractions (r = 1. 98, 3.96, 7.92, 14.8) and reacted for 48 h to obtain a polyamide acid (PAA) solution as a precursor.[6] The solution was spin-coated onto a fused silica substrate, dried at 70°C for 20 min, and thermally imidized at 220°C for 1.5 h under nitrogen flow to obtain end-capped PI (ODDC-TsAPA) films. The completion of imidization was characterized by ATR-FT-IR spectra.

3. Results and Discussion

Figure 3 shows the UV-vis absorption/emission spectra of the ODDC-TsAPA thin films, the r-dependence of the fluorescence colour under white or UV light irradiation, and the chromaticity diagram of the emission colour of each thin film. All PI films were colourless and transparent under white light, absorbed UV light, and presented purple to orange fluorescence. The intensity of the peak at 400 nm in the emission spectrum, which is attributable to the fluorescence of the ODDC of the main chain, decreased with an increase in r. On the other hand, the peak intensities at 450 nm and 585 nm increased with increasing r, and these peaks are attributable to the fluorescence wmitted from 3TsAPA introduced at the PI termini. Given that the fluorescence wavelengths of the A*and T* forms of 3TsAPI in solution are approximately 500 nm and 600 nm, respectively, the fluorescence at 450 nm and 585 nm were attributable to the A*and T* forms of 3TsAPA, respectively. The fluorescence lifetime of the ODDC component of the main chain was measured, and the Förster-type resonance energy transfer (FRET) efficiency (E_{FRET}) from the main chain to the end was evaluated by equation (1), where $\tau_{\mathrm{ODDC\text{-}TsAPA}}$ is the lifetime of ODDC in ODDC-TsAPA thin films, and τ_{ODDC} is that of ODDC homopolymer. **Table 1** summarizes the resultant τ and E_{FRET} values.

$$E_{\mathrm{FRET}} = \frac{\tau_{\mathrm{ODDC}} - \tau_{\mathrm{ODDC-TsAPA}}}{\tau_{\mathrm{ODDC}}} \qquad (1)$$

Table 1 (right) Fluorescence lifetimes (τ) and FRET efficiencies (E_{FRET}) of ODDC-TsA prepared with variable r

	ODDC	**1.98**	**3.96**	**7.92**	**14.8**
τ (ns)	10.10	4.91	3.04	2.49	1.83
E_{FRET}	-	0.51	0.70	0.75	0.82

With increasing the end-group fraction r, E_{FRET} significantly increased, possibly due to the increased concentration of end-groups, which shortened the spatial distance between the donor (ODDC) and acceptor (3TsAPA) and facilitated energy transfer by FRET. In the thin film with the highest end-group fraction (r = 14.8), E_{FRET} reached 82 %, which resulted in a higher intensity of orange fluorescence via ESIPT than the blue fluorescence from the main chain, even though 3TsAPA was introduced only at the chain ends.

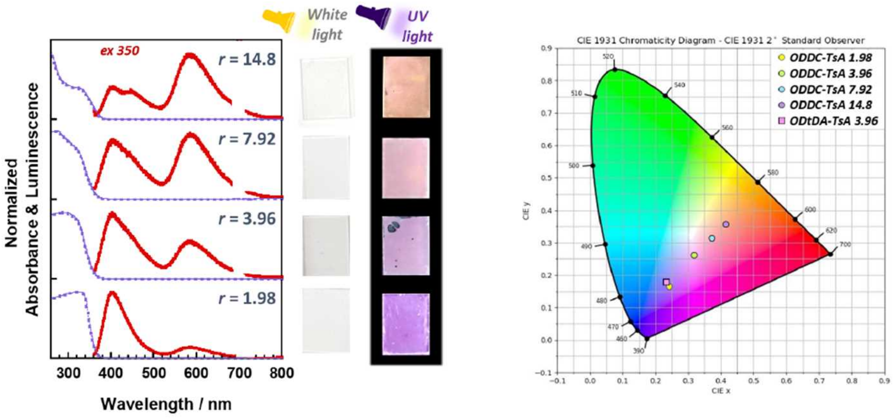

Figure 3 UV–vis absorption and emission spectra and CIE coordinates of ODDC-TsA (λ_{ex} = 350 nm), which were prepared with variable *r* values, and photographs of these films under white light (UV off) and UV (λ = 365 nm) irradiation (UV on).

Normalised fluorescence spectra obtained by varying the UV wavelength irradiating the thin films by 10 nm in the range 330-400 nm are shown in **Figure 4** with the chromaticity diagram in **Figure 5**. It should be noted that the shape of the spectra and the emission colour varied with the excitation wavelength. At λ_{ex} = 330 nm, dual fluorescence was observed, with those at about 400 nm from ODDC and at about 580 nm from the T* form of 3TsAPA; when λ_{ex} was increased to 350 nm, the relative intensity of the T*-derived fluorescence to that of ODDC increased. When λ_{ex} was further increased to 400 nm, the fluorescence peak wavelength shifted to approximately 460 nm.

The photophysical processes of ODDC-TsAPA, deduced from the facts that the λ_{ex} of ODDC is 344 nm and the optimum λ_{ex} of 3TsAPI is 370 nm in the crystalline state and 350 nm in $CHCl_3$, are summarised in **Figure 6** for each excitation wavelength. Short excitation wavelengths are close to the optimum λ_{ex} of ODDC, so there is competition between **a)** ODDC blue fluorescence, **b)** A*-type blue-green fluorescence via FRET from ODDC to the A*-type of 3TsAPA, and **c)** T*-type red fluorescence via FRET to the N*-type and subsequent ESIPT. As the medium excitation wavelength is close to the excitation wavelength of 3TsAPI, it is likely that in addition to a) ODDC fluorescence, **d)** direct excitation of the terminal 3TsAPA, resulting in enhanced T*-type fluorescence. Finally, long-wavelength excitation cannot excite the ODDC or T*types, thus, **e)** the A-type was directly excited, resulting in A*type fluorescence. The above results clarified that the mixing ratio of the three types (ODDC, T*-type, and A*-type) of fluorescence can be controlled by adjusting *r* and λ_{ex} to obtain a relatively wide range of emission colours in the ODDC-TsAPA thin films.

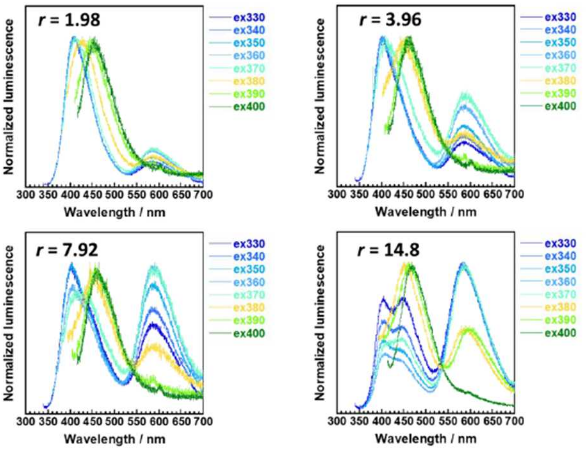

Fig. 4 Normalized fluorescence spectra of ODDC-TsAPA (*r* = 1.98, 3.96, 7.92, 14.8) observed with different excitation wavelengths (λ_{ex} = 330, 340, 350, 360, 370, 380, 390, and 400 nm).

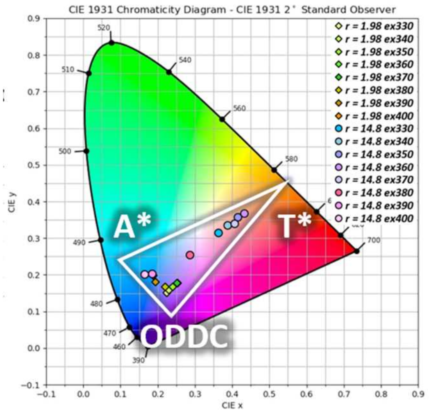

Fig. 5 CIE coordinates of the fluorescence colors of ODDC-TsAPA at different excitation wavelengths with *r* = 1.98, 14.8.

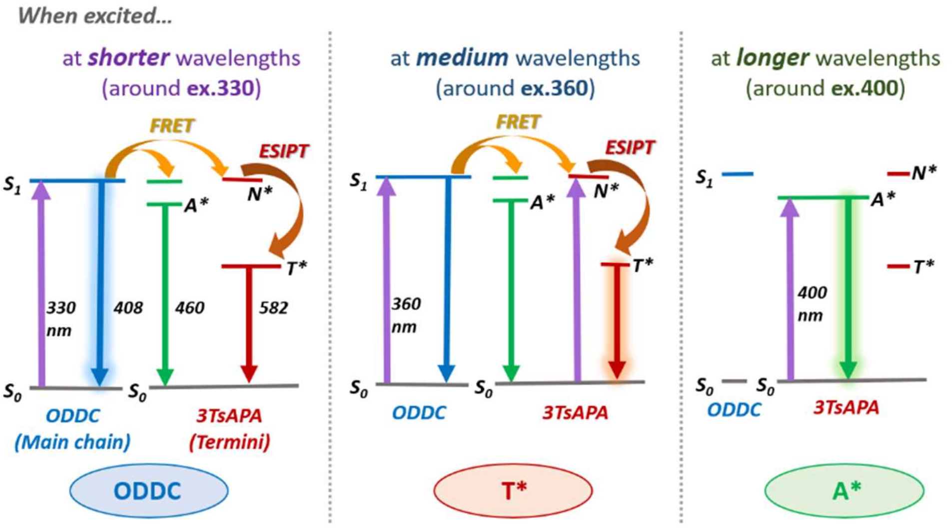

Fig. 6 Diagrams of the photophysical processes of ODDC-TsAPA excited at shorter (left), medium (centre), and longer wavelengths (right).

Furthermore, when a PI thin film with *r* = 14.8 was exposed to trifluoroacetic acid (TFA) vapor, the fluorescence colour changed from orange to light blue (**Figure 7**), which is due to the formation of hydrogen bonds between TFA and 3TsAPA, which generates the N* form and suppresses ESIPT. Further exposure to triethylamine basic vapour changed the fluorescent colour to green, which is due to the formation of the A* form. However, additional washing by water could not restore the original orange fluorescence, and the film has detached from the substrate. The successful fabrication of fluorescent PI films with a wide range of emission colours in response to the ambient atmosphere is expected to lead to environmental sensor applications.

Finally, TGA measurements showed that the 5% weight loss temperature was above 430 °C for all films (**Figure 8**), indicating that the PI films have sufficient thermal stability for optical and electronic applications.

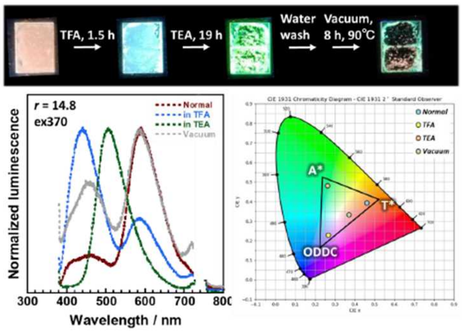

Figure 7 Normalized fluorescence spectra of 1) ODDC-TsAPA PI film (λ_{ex} = 370 nm) prepared with *r* = 14.8, 2) exposed to TFA, 3) followed by exposure to TEA, and 4) finally washed with water, and the photographs of those films under UV (λ = 365 nm) irradiation and its CIE coordinates.

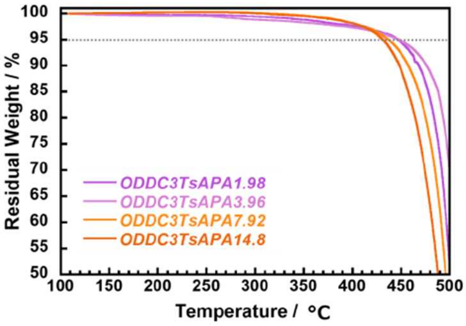

Figure 8 Thermogravimetric analyses (TGA) for ODDC-TsAPA films prepared with variable *r* values (*r* = 1.98, 3.96, 7.98, 14.8).

4. Conclusion

A novel acid anhydride 3TsAPA with a chemical structure similar to that of imide compounds exhibiting multi-colour fluorescence in solution has been synthesised, and end-capped PI (ODDC-TsAPA) has been developed by introducing it into both ends of a blue fluorescent PI,ODDC. ODDC-TsAPA is a colourless, transparent thin film, and it exhibits a wide range of fluorescence colours from purple to orange under UV irradiation by adjusting the fraction of end-group (*r*). This multi-colour fluorescence is induced by the highly efficient energy transfer from the ODDC main chain to the 3TsAPA termini (E_{FRET} =82 % at *r* =14.8). The fluorescence spectrum of ODDC-TsAPA gradually changed depending on the excitation wavelength. At the shorter excitation wavelengths, ODDC main chain is excited, and it emits N*-type fluorescence. At medium excitation wavelengths, T*-type fluorescence is also emitted from the 3TsAPA termini via ESIPT from N*. At the longer excitation wavelengths, only anion(A*)-type fluorescence is emitted from the deprotonated 3TsAPA termini. Therefore, the intensities of the fluorescence from the ODDC, T* and A* states change by adjusting *r* and excitation wavelength, which results in a wide range of emission colours. In addition, when the PI films were exposed to vapours of organic acid (TFA) and base (DBU), their emission colours changed from orange by T* form to blue and green due to the formation of N*and A* forms of 3TsAPA, respectively.

In conclusion, by introducing a multi-coloured fluorescent moiety (3TsAPA), which is an extremely efficient acceptor for energy transfer from the main chain, into the PI termini, we have succeeded in developing thin films that exhibit multi-coloured fluorescence dependent on the excitation wavelength as well as the polarity of the surrounding environment, while maintaining the high thermostability derived from the structural rigidity of the PIs. The molecular design of the main chain and the end groups that induces highly efficient FRET is essential to obtain thin films with such properties; the resultant ODDC-TsAPA PI is expected to be applied to thermally stable environmental response sensors that detect vapours of organic acids and bases.

References

1. Wakita, J., Sekino, H., Sakai, K., Urano, Y. & Ando, S. Molecular Design, Synthesis, and Properties of Highly Fluorescent Polyimides. *J. Phys. Chem. B* **113,** 15212–15224 (2009).
2. Wakita, J., Inoue, S., Kawanishi, N. & Ando, S. Excited-state intramolecular proton transfer in imide compounds and its application to control the emission colors of highly fluorescent polyimides. *Macromolecules* **43,** 3594–3605 (2010).
3. Fujiwara, E., Orita, R., Vyšniauskas, A., Franckevičius, M., Ishige, R., Gulbinas, V. & Ando, S. Ultrafast Spectroscopic Analysis of Pressure-Induced Variations of Excited-State Energy and Intramolecular Proton Transfer in Semi-Aliphatic Polyimide Films. *J. Phys. Chem. B* **125,** 2425–2434 (2021).
4. Tabuchi, A., Hayakawa, T., Kuwata, S., Ishige, R. & Ando, S. Full-colour solvatochromic fluorescence emitted from a semi-aromatic imide compound based on ESIPT and anion formation. *Mater. Adv.* **2,** 5629–5638 (2021).
5. Liang, N., Fujiwara, E., Nara, M., Ishige, R. & Ando, S. Colorless Copolyimide Films Exhibiting Large Stokes-Shifted Photoluminescence Applicable for Spectral Conversion. *ACS Appl. Polym. Mater.* **3,** 3911–3921 (2021).
6. Tabuchi, A., Hayakawa, T., Kuwata, S., Ishige, R. & Ando, S. Synthesis and Characterization of White-Light Luminescent End-Capped Polyimides Based on FRET and Excited State Intramolecular Proton Transfer. *Polymers (Basel).* **13,** 4050 (2021).
7. Liang, N., Kuwata, S., Ishige, R. & Ando, S. Large-Stokes-shifted yellow photoluminescence emission from an imide and polyimides forming multiple intramolecular hydrogen bonds. *Mater. Chem. Front.* **6,** 24–32 (2022).
8. Takizawa, K., Wakita, J., Sekiguchi, K. & Ando, S. Variations in aggregation structures and fluorescence properties of a semialiphatic fluorinated polyimide induced by very high pressure. *Macromolecules* **45,** 4764–4771 (2012).
9. Kanosue, K. & Ando, S. Fluorescence emissions of imide compounds and end-capped polyimides enhanced by intramolecular double hydrogen bonds. *Phys. Chem. Chem. Phys.* **17,** 30659–30669 (2015).
10. Kanosue, K., Shimosaka, T., Wakita, J. & Ando, S. Polyimide and Imide Compound Exhibiting Bright Red Fluorescence with Very Large Stokes Shifts via Excited-State Intramolecular Proton Transfer. *Macromolecules* **48,** 1777–1785 (2015).

11. Kanosue, K., Augulis, R., Peckus, D., Karpicz, R., Tamulevičius, T., Tamulevičius, S., Gulbinas, V. & Ando, S. Polyimide and Imide Compound Exhibiting Bright Red Fluorescence with Very Large Stokes Shifts via Excited-State Intramolecular Proton Transfer II. Ultrafast Proton Transfer Dynamics in the Excited State. *Macromolecules* **49,** 1848–1857 (2016).
12. Orita, R., Franckevičius, M., Vyšniauskas, A., Gulbinas, V., Sugiyama, H., Uekusa, H., Kanosue, K., Ishige, R. & Ando, S. Enhanced fluorescence of phthalimide compounds induced by the incorporation of electron-donating alicyclic amino groups. *Phys. Chem. Chem. Phys.* **20,** 16033–16044 (2018).
13. Liang, N., Fujiwara, E., Nara, M., Ishige, R. & Ando, S. Photoluminescence Properties of Novel Fluorescent Polyimide Based on Excited State Intramolecular Proton Transfer at The End Groups. *J. Photopolym. Sci. Technol.* **32,** 449–455 (2019).
14. Kanosue, K., Hirata, S., Vacha, M., Augulis, R., Gulbinas, V., Ishige, R. & Ando, S. A colorless semi-aromatic polyimide derived from a sterically hindered bromine-substituted dianhydride exhibiting dual fluorescence and phosphorescence emission. *Mater. Chem. Front.* **3,** 39–49 (2019).
15. Nara, M., Orita, R., Ishige, R. & Ando, S. White-Light Emission and Tunable Luminescence Colors of Polyimide Copolymers Based on FRET and Room-Temperature Phosphorescence. *ACS Omega* **5,** 14831–14841 (2020).